Solar Energy Materials & Solar Cells 95 (2011) 2848–2854

Contents lists available at ScienceDirect

Solar Energy Materials & Solar Cells

journal homepage: www.elsevier.com/locate/solmat

Absorption coefficient of bulk and thin film Cu_2O

Claudia Malerba [a,b], Francesco Biccari [a,*], Cristy Leonor Azanza Ricardo [b], Mirco D'Incau [b], Paolo Scardi [b], Alberto Mittiga [a]

[a] ENEA, Casaccia Research Center, via Anguillarese 301, 00123 Roma, Italy
[b] Department of Materials Engineering and Industrial Technologies, University of Trento, via Mesiano 77, 38123 Trento, Italy

ARTICLE INFO

Article history:
Received 1 March 2011
Accepted 25 May 2011
Available online 23 June 2011

Keywords:
Cu_2O
Cuprous oxide
Optical properties
Exciton absorption

ABSTRACT

The optical absorption coefficient of thin film and bulk Cu_2O at room temperature is obtained from an accurate analysis of their transmittance and reflectance spectra. These absorption spectra are modeled, together with the low temperature data reported in the literature, using an analytical expression to assess and quantify the role of the different absorption mechanisms. The results suggest that direct forbidden transitions and indirect transitions play an almost equally relevant role. A table of the optical constants of Cu_2O single crystal is given for reference.

© 2011 Elsevier B.V. All rights reserved.

1. Introduction

Cu_2O has recently attracted much attention for many different applications (photocatalytic water splitting [1], thin film transistors [2], resistive random access memory [3], spintronic devices [4]) but it was investigated for many decades since it has been always considered a good material for the fabrication of photovoltaic devices.

So far the best performing solar cells were fabricated on Cu_2O substrates obtained by high temperature oxidation of copper sheets [5], but their fill factor (*FF*) is still limited by the low electric conductivity of the thick Cu_2O substrates. Thin film structures could solve this problem and, also, avoid the use of large quantities of high purity copper. However Cu_2O thin film solar cells have always shown poor performances: the best cell obtained by reactive rf magnetron sputtering [6] reached $V_{oc}=0.26$ V, $J_{sc}=2.8$ mA/cm^2, $FF=0.55$ giving a conversion efficiency equal to 0.4%. A similar result was achieved for electrodeposited devices. These devices show a low quantum efficiency (QE) for $\lambda>500$ nm, as a consequence of a small diffusion length (L_D) of the minority carriers [7]. The fit of the quantum efficiency to deduce L_D is an important tool for the device optimization and a good knowledge of the material absorption coefficient $\alpha(\hbar\omega)$ is necessary.

The behavior of the absorption coefficient of cuprous oxide is rather spectacular, especially at low temperatures where the contribution of four exciton series (*yellow*, *green*, *blue* and *violet*) is quite evident and it was measured and analyzed by many different authors [8–10].

The theory of optical absorption by excitons in semiconductors was developed by Elliott in 1957 [11] taking into account the exciton bound states as well as the Coulomb interaction on the unbound hole–electron pairs. This theory was able to explain the main features of cuprous oxide absorption spectra, demonstrating that Cu_2O is a semiconductor with a direct forbidden energy gap ($E_g=2.09$ eV at room temperature).

At room temperature the absorption coefficient was obtained by spectrophotometric measurements up to 2.4 eV, whereas optical constants at higher energies were more recently obtained by ellipsometry [12]. However, these two sets of measurements do not match properly, and therefore experimental data for Cu_2O absorption coefficient are not available in the whole energy range of interest.

Several works were devoted to the analysis of the transmittance and reflectance spectra of thin Cu_2O thin films. In these works $\alpha(\hbar\omega)$ is derived in order to measure the optical gap of the film and to check that only the desired Cu_2O phase is present. The results obtained from these analyses show an amazing variability partly due to the use of unsatisfactory procedures for removing the interference fringes but also to the fact that data analysis was made in different ways by the various authors.

For Cu_2O, a semiconductor with a direct forbidden gap, it would be reasonable to assume that, at room temperature, in the energy range between 2.09 eV (E_g) and 2.64 eV (i.e. the lowest direct allowed optical gap), $\alpha(\hbar\omega)$ behaves as $(\hbar\omega-E_g)^{3/2}$. As a consequence, E_g should be obtained by a linear fit on a plot of $(\alpha\hbar\omega)^{2/3}$. However quite often this simple approach is not used, and many authors use instead an $(\alpha\hbar\omega)^2$ plot [13,14] which is the behavior expected for direct allowed gap semiconductors. As a result, widely different gap values were reported (from 2.16 [14] to 2.5 eV [13]).

In the present article we show that even the linear fit of $(\alpha\hbar\omega)^{2/3}$ versus $\hbar\omega$ is not appropriate, as above the gap the absorption coefficient is given by a superposition of several different absorption mechanisms. In particular, we present a

* Corresponding author. Tel.: +39 06 3048 4214; fax: +39 06 3048 6405.
E-mail addresses: biccari@gmail.com, francesco.biccari@enea.it (F. Biccari).

0927-0248/$ - see front matter © 2011 Elsevier B.V. All rights reserved.
doi:10.1016/j.solmat.2011.05.047

detailed analysis of the Cu_2O absorption coefficient showing that, in the energy region just above E_g, there are important contributions from the direct forbidden transitions toward green exciton states and from indirect transitions.

2. Review of optical absorption by excitons in Cu_2O

The Cu_2O absorption properties are strongly dependent on excitonic effects. Many works reported in the literature have shown that the absorption spectra arising from the yellow and the green excitons in Cu_2O are in good agreement with Elliott's theory [11]. In his theory, Elliott considers a simple model of a direct gap semiconductor where the exciton is formed by an electron and a hole from two spherical and non-degenerate bands, with wave vectors $\boldsymbol{k}_e$ and $\boldsymbol{k}_h$ and effective masses m_e and m_h, respectively.

The energies of the bound states are

$$E_n = E_g + \frac{\hbar^2 \boldsymbol{K}^2}{2M} - \frac{R_{ex}}{n^2}, \tag{1}$$

where $\boldsymbol{K} = \boldsymbol{k}_e + \boldsymbol{k}_h$, $M = m_e + m_h$, $R_{ex} = \mu e^4/(2\varepsilon^2\hbar^2(4\pi\varepsilon_0)^2)$ and where the reduced mass is $\mu = m_e m_h/(m_e + m_h)$. The effective Bohr radius is $a = 4\pi\varepsilon_0\hbar^2\varepsilon/(\mu e^2)$.

For unbound states, instead, the energy is

$$E_{\boldsymbol{k}_r} = E_g + \frac{\hbar^2 \boldsymbol{K}^2}{2M} + \frac{\hbar^2 \boldsymbol{k}_r^2}{2\mu}, \tag{2}$$

where $\boldsymbol{k}_r = (m_h\boldsymbol{k}_e - m_e\boldsymbol{k}_h)/(m_e + m_h)$.

It is worth noting that the energy of the 1s level does not follow Eq. (1) and it is split by the exchange interaction in ortho and para components. Since this interaction depends on the probability of finding electron and hole in the same unit cell, it is nonzero only for states with s-like envelope [15].

2.1. Direct forbidden transitions

Because of momentum conservation, the only transitions which can take place from the ground state of the semiconductor (state $|0\rangle$) are those toward the exciton's states with $\boldsymbol{K} = \boldsymbol{0}$, i.e. $\boldsymbol{k}_e = -\boldsymbol{k}_h$. Therefore, there will be a line spectrum corresponding to the creation of excitons with $\boldsymbol{K} = \boldsymbol{0}$ in different excited states, followed by a continuous absorption corresponding to the creation of unbound but interacting hole–electron pairs.

For a direct transition from the ground state $|0\rangle$ toward a single discrete level $|\boldsymbol{K},n\rangle$ of energy 0 and E_n, respectively, the absorption coefficient can be written as

$$\alpha = \frac{\pi\hbar^2 e^2}{c\eta\varepsilon_0\omega m_0^2}|M_{n0}|^2\delta(E_n - \hbar\omega)\tilde{N} = \frac{\pi\hbar e^2}{2c\varepsilon_0 m_0}\frac{f_n}{\eta}\delta(E_n - \hbar\omega)\tilde{N}, \tag{3}$$

where $M_{n0} = \langle \boldsymbol{K},n|\boldsymbol{\xi}\cdot\boldsymbol{\nabla}e^{i\boldsymbol{q}\cdot\boldsymbol{r}}|0\rangle$, $\boldsymbol{\xi}$ is the polarization unit vector of the potential vector $\boldsymbol{A}$, m_0 is the free electron mass, $\boldsymbol{q}$ is the photon momentum, η is the refractive index and $\tilde{N}$ is the number of elementary cells per unit volume. In the last expression we have used the definition of the oscillator strength

$$f_n = \frac{2\hbar}{\omega m_0}|M_{n0}|^2. \tag{4}$$

The value of f_n/η can be found from the experimental data [8] by integrating the peak absorption over $\hbar\omega$

$$\frac{f_n}{\eta} = \frac{2cm_0\varepsilon_0}{\pi\hbar e^2\tilde{N}}\int \alpha(\hbar\omega)\, d(\hbar\omega). \tag{5}$$

In the case of a continuous distribution of final states, the absorption coefficient results from the integration of Eq. (3) over their distribution:

$$\alpha = \frac{\pi\hbar^2 e^2}{c\eta\varepsilon_0\omega m_0^2}|M_{n0}|^2 S_n(\hbar\omega), \tag{6}$$

where $S_n(\hbar\omega)$ is the density of states per unit energy and unit volume.[1] Eq. (6) will be used to describe both the pseudo-continuous absorption just below the gap, due to the overlap of the exciton lines at large n, and the true continuous absorption above the energy gap (where n should be replaced by $\boldsymbol{k}_r$).

Using the oscillator strength, the absorption coefficient can be expressed as

$$\alpha = \frac{\pi\hbar e^2}{2c\varepsilon_0 m_0}\frac{f_n}{\eta}S_n(\hbar\omega). \tag{7}$$

Using this formula we can describe the absorption coefficient behavior in the small energy range just below the gap where the exciton lines overlap (pseudo-continuous absorption). In this case the density of states can be approximated by

$$S_n(\hbar\omega) = \tilde{N}\left(\frac{\partial}{\partial n}\frac{R_{ex}}{n^2}\right)^{-1} = \tilde{N}\left(\frac{2R_{ex}}{n^3}\right)^{-1} = \frac{\tilde{N}R_{ex}^{1/2}}{2(E_g - \hbar\omega)^{3/2}}. \tag{8}$$

For direct forbidden transitions towards bound states the oscillator strength is [11]

$$f_n = b\frac{n^2 - 1}{n^5}, \tag{9}$$

where $b = Bgx^4/(3\pi a^5)$, $g = 2m_0\omega/\hbar$, $B = 1/\tilde{N}$ is the volume of the elementary unit cell and x is the position matrix element calculated between the electron and the hole states. Its value is roughly equal to an atomic radius. In the case of one or both degenerate bands, the matrix element x has to be replaced by $\sum_{jj'}x_{jj'}$, where j and j' are two labels for the electron and hole bands.

From the previous argument it is possible to write f_n as a function of f_2

$$f_n = \frac{32}{3}f_2\frac{\hbar\omega}{\hbar\omega_2}\frac{n^2 - 1}{n^5}, \tag{10}$$

where $\hbar\omega_2 = R_{ex}/4$. From Eqs. (7) and (10), using $n^2 = R_{ex}/(E_g - \hbar\omega)$ and the fine structure constant $\tilde{\alpha} = e^2/(4\pi\varepsilon_0\hbar c)$, we obtain the final result

$$\alpha^{bound} = \left(\frac{32\pi^2\hbar^2\tilde{\alpha}}{3m_0R_{ex}B}\right)\frac{f_2}{\eta}\frac{\hbar\omega}{\hbar\omega_2}\left(1 - \frac{E_g - \hbar\omega}{R_{ex}}\right) \tag{11}$$

or, in a different form,

$$\alpha^{bound} = A\frac{\hbar\omega}{\hbar\omega_2}\left(1 - \frac{E_g - \hbar\omega}{R_{ex}}\right), \tag{12}$$

where

$$A = \frac{32\pi^2\hbar^2\tilde{\alpha}}{3m_0R_{ex}B}\frac{f_2}{\eta} = \frac{2\pi\tilde{\alpha}x^4(2\mu)^{5/2}R_{ex}^{3/2}}{3\eta\hbar^5}\hbar\omega_2. \tag{13}$$

In the case of degenerate bands, the right hand side of this expression has to be multiplied by a factor equal to this degeneracy.[2]

[1] Eq. (6) is equivalent to Elliott's equation (3.4) in which $\sigma = e^{i\boldsymbol{q}\cdot\boldsymbol{r}}\boldsymbol{\xi}\cdot\boldsymbol{j}$, $\boldsymbol{j}$ is the current operator acting on electron states and where c.g.s. units are used. Note that in Elliott's work the refractive index is omitted.

[2] Note that Eqs. (12) and (13) are equivalent to the Elliott formula (3.17), obtained using $\varepsilon = e^2/(2aR_{ex}4\pi\varepsilon_0)$, apart from the dimensionless factor N (number of the elementary cells in the crystal) which comes from the normalization of the wave function used by the author.

For direct forbidden transitions toward the unbound states, Elliott's theory [11] predicts an absorption coefficient

$$\alpha^{\text{unbound}} = \frac{\pi\omega\tilde{\alpha}x^4(2\mu)^{5/2}}{3\eta\hbar^4}\cdot\frac{\beta(1+\beta^2)\,e^{\pi\beta}}{\sinh(\pi\beta)}(\hbar\omega-E_g)^{3/2}, \tag{14}$$

where

$$\beta = \left(\frac{R_{ex}}{\hbar\omega-E_g}\right)^{1/2}. \tag{15}$$

Eq. (14) can be rewritten in a different form, using the same constant A introduced for the pseudo-continuous absorption:

$$\alpha^{\text{unbound}} = \frac{A\hbar\omega}{R_{ex}\hbar\omega_2}\cdot\frac{1}{1-e^{-2\pi\beta}}(\hbar\omega-E_g+R_{ex}), \tag{16}$$

where we have used

$$\beta(1+\beta^2)(\hbar\omega-E_g)^{3/2} = R_{ex}^{1/2}(\hbar\omega-E_g+R_{ex}). \tag{17}$$

It is easy to verify that α^{unbound} and α^{bound} join when $\hbar\omega\to E_g$ and their limit value is $AE_g/(\hbar\omega_2)$. On the other hand, when $\hbar\omega\to\infty$, the absorption coefficient varies like $(\hbar\omega-E_g)^{3/2}$, in agreement with the theory for direct forbidden gap semiconductors without excitonic effects.

In addition to the yellow and the green exciton series, two more excitonic spectra, the blue and the violet ones, are reported for Cu_2O. These two last series are in good agreement with Elliott's theory for direct allowed transitions, but their contributions to the optical absorption has to be taken into account only in the high energy region, which nevertheless, even in the case of thin films, is usually outside the typical energy range of the spectrophotometric data. However, in the higher energy region of the absorption spectrum at room temperature, because of the broadening of the exciton lines, there is a contribution arising from the allowed transitions toward the blue and violet $n=1$ exciton levels. This last contribution will be taken into account in the discussion of our experimental data.

2.2. Indirect transitions

The theory of direct forbidden transitions predicts that the $n=1$ line is missing (see Eq. (9)) but the transition toward this excitonic level can take place as an indirect one, with the absorption or the emission of one phonon, supposed to belong to a flat optical branch of constant energy E_{ph}. In this case the absorption coefficient in the dipole approximation is given by [16]:

$$\alpha = \frac{\pi\hbar^2e^2}{c\eta\varepsilon_0\omega m_0^2}\left|\sum_i\frac{\langle 1s,\boldsymbol{K};n_k\pm1|H_{e-ph}|i,\boldsymbol{0}\rangle\langle i,\boldsymbol{0}|\boldsymbol{\xi}\cdot\boldsymbol{\nabla}|0\rangle}{E(i,\boldsymbol{0})-E(1s,\boldsymbol{K})\mp E_{ph}}\right|^2 S_{1s}(\hbar\omega), \tag{18}$$

where H_{e-ph} is the electron–phonon interaction operator and where the sum runs over all the possible virtual transitions (which conserve wavevector but not energy) to the intermediate states $|i,0\rangle$.

The final density of states $S_{1s}(\hbar\omega)$ in the exciton band is proportional to $(\hbar\omega-E(1s,\boldsymbol{0}))^{1/2}$. Therefore, if the matrix elements and the denominators are approximately constant, α is given by

$$\alpha = C_{abs}(\hbar\omega-E_g+E_b+E_{ph})^{1/2}+C_{em}(\hbar\omega-E_g+E_b-E_{ph})^{1/2}, \tag{19}$$

where $E_b=E_g-E(1s,\boldsymbol{0})$ is the exciton binding energy and C_{abs} and C_{em} are two coefficients for the absorption and emission transitions which can be expressed as

$$C_{abs}=CN,\quad C_{em}=C(N+1), \tag{20}$$

where

$$N=\frac{1}{e^{E_{ph}/(kT)}-1}, \tag{21}$$

C is a constant independent of the temperature in a first approximation and N is the mean occupation number of the phonon level.

Symmetry considerations [17] show that the phonons involved in transitions to the ortho-1s yellow level must belong to the following four symmetries: Γ_{25}^-, Γ_{12}^-, Γ_{15}^-, Γ_2^-. The indirect transitions to the ortho-1s level of the yellow exciton were resolved, for example, using wavelength modulation techniques identifying five different phonons and obtaining the transition intensities and broadening parameters at 4.2 K [18].

A similar study on the indirect transitions to the ortho-1s state of the green exciton is more difficult since their edges fall within the energy region of the yellow series. Forman [19] claims that the indirect absorption to the ortho-1s state of the green exciton with the emission of a 19 meV Γ_{15}^- phonon constitutes, at 20 K, a large contribution to the background of the yellow series and to the absorption continuum above it. A possible alternative explanation was put forward by Agekyan [20], who suggested the possibility that the observed absorption is due to indirect transition to the yellow exciton states with $n\geq2$. On the other hand according to Matsuura [21] the indirect transitions toward p states should be very weak and therefore not observable.

Indeed, we will show in the next paragraph that a good fit can be obtained without introducing indirect transitions to the p states, in agreement with Forman's hypothesis, even if our analysis suggests that the involved phonon is not the 19 meV Γ_{15}^- but the 43.4 meV Γ_2^-.

3. Fit of low temperature absorption data

Experimental data can be modeled by Eqs. (12) and (16) provided that the oscillator strengths for the direct transition to the level 2p of the yellow and green series are given. These values can be found integrating the peak absorption using the experimental data taken at low temperature (4 and 77 K) where the peaks of the p states are clearly visible. Therefore we tried to calculate the A constants using the $n=2$ oscillator strength $f_2^y/\eta=1.02\times10^{-6}$ [8] and $f_2^g/\eta=1.16\times10^{-5}$ reported in the literature [9]. The A constant values were obtained from Eq. (13) using $B=(4.26\times10^{-8})^3\ \text{cm}^3$, the Rydberg constants $R_{ex}^y=97.43$ meV and $R_{ex}^g=149.7$ meV [9]. The resulting values for the constant were $A^y=78.5\ \text{cm}^{-1}$ and $A^g=585\ \text{cm}^{-1}$.

It turns out that the value for the green exciton is too low to give satisfactory results and it must be noted that even lower values were obtained by other authors [22,23]. We have therefore reexamined the procedure used to derive f_2^g/η, recognizing that the result critically depends on the background subtraction and on the function used to describe the peak shape. All authors [22–24] adopt a smooth and arbitrary background, which connects the continuous absorption at lower and higher energies passing through the peak minima and an asymmetric Lorentzian to describe the broadened and asymmetric peak. The asymmetric Lorentzian is predicted by Toyozawa's theory [25] and produces, at energies somewhat larger than the maximum, a negative dip followed by a negative tail. The use of such a function gives good results for the yellow series, where the dip just above the maxima is indeed observed. The fit quality obtained for the green series is instead not as good and moreover it can be easily checked that the numerical value reported by Grun and Nikitine [24] is inconsistent even with the expression used in that same paper to fit the data (using the formula adopted in [24] the value should be instead $f_2^g/\eta=1.64\times10^{-5}$).

We have therefore performed a new data analysis trying to fit the absorption spectrum [26] as a whole. In this way we can obtain more reliable values of the f/η values and also obtain information about the intensity of the different indirect absorption processes which are easier to individuate at low temperatures.

For the indirect transitions to the ortho-1s yellow level we have included only the two strongest processes [27] (involving the 13.6 meV Γ_{12}^- and the 82 meV Γ_{15}^- phonons). For the indirect transitions to the ortho-1s green level the best results are obtained considering the 13.6 meV Γ_{12}^- and the 43.4 meV Γ_2^- phonons. It must be noted that the ortho-1s green exciton is located about 43 meV below the lowest conduction band. Therefore, for the virtual state obtained by exciting an electron in this band, the denominator in Eq. (18) is very small for the process involving the emission of a 43.4 meV Γ_2^- phonon. This explains why this transition is the strongest.

The binding energy values of the ortho-1s yellow (E_b^y) [28] and green (E_b^g) [29] excitons are reported in Table 1 and it is worth noting that, as explained in Section 2, they are different from the Rydberg values of the corresponding peak series. The energy gap values reported in Table 1 were calculated from the expressions given in [27].

The yellow and green line spectrum and the continuous absorption above their gap are described using only the two parameters f_2^y/η and f_2^g/η. The continuous contributions due to the yellow and the green excitons have been evaluated according to Eq. (16).

The yellow series peaks were modeled by the usual asymmetric Lorentzian functions. The same approach cannot be followed for the green series as the overlap of the negative tails would give a very low absorption near the gap in complete disagreement with the experimental data. The green series peaks were therefore fitted using symmetric Lorentzian functions.

We found that using $f_2^y/\eta = 1.02\times10^{-6}$ and $f_2^g/\eta = 2.25\times10^{-5}$ the peak intensities and the continuous absorptions can be reproduced fairly well. Therefore we see that the f_2^y/η value is equal to the usual one [8] whereas for the green series the f_2^g/η value is almost twice the literature value. The resulting values for the constant were $A^y = 78.5\ \mathrm{cm}^{-1}$ and $A^g = 1115\ \mathrm{cm}^{-1}$. The result of the fit is shown in Fig. 1.

With these values the experimental ratio $f_2^g/f_2^y = 21.8$ is obtained: this number must be compared with the theoretical expression $f_2^g/f_2^y = 2(R^g/R^y)^5 = 17.15$ where the factor 2 is due to the two-fold degeneracy of the green exciton [27].

Table 1
Values of the parameters used to fit $\alpha(\hbar\omega)$ at three different temperatures. The only adjustable parameters are the C constants which describe the intensities of the indirect transitions.

$R_{ex}^y = 0.09743$ eV		$R_{ex}^g = 0.1497$ eV	
$E_b^y = E_g^y - E_{ortho}^y(1s,\mathbf{0}) = 0.1393$ eV		$E_b^g = E_g^g - E_{ortho}^g(1s,\mathbf{0}) = 0.177$ eV	
$f_2^y/\eta = 1.02\times10^{-6}$		$f_2^g/\eta = 2.25\times10^{-5}$	
$B = 7.731\times10^{-23}\ \mathrm{cm}^3$			
	$T=4$ K	$T=77$ K	$T=293$ K
E_g^y (eV)	2.173	2.164	2.094
E_g^g (eV)	2.304	2.294	2.225
$C_{1s}^y(\Gamma_{12}^-)$ ($\mathrm{cm}^{-1}\ \mathrm{eV}^{-1/2}$)	380	380	380
$C_{1s}^y(\Gamma_{15}^-)$ ($\mathrm{cm}^{-1}\ \mathrm{eV}^{-1/2}$)	62	62	62
$C_{1s}^g(\Gamma_{12}^-)$ ($\mathrm{cm}^{-1}\ \mathrm{eV}^{-1/2}$)	400	500	700
$C_{1s}^g(\Gamma_2^-)$ ($\mathrm{cm}^{-1}\ \mathrm{eV}^{-1/2}$)	1600	1800	3200
N(13.6 meV Γ_{12}^-)	~0	0.148	0.98
N(43.4 meV Γ_2^-)	~0	1.45×10^{-3}	0.23
N(82 meV Γ_{15}^-)	~0	5.85×10^{-6}	0.047

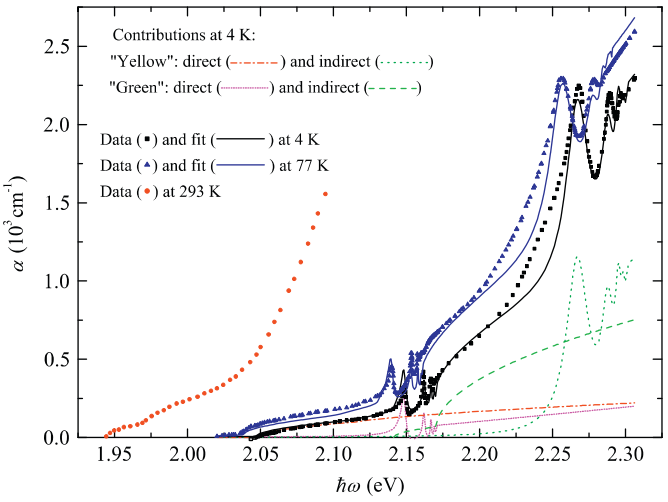

Fig. 1. Absorption coefficient data obtained on a 10 μm thick bulk sample by Grun et al. [26] at 293 K (dots), 77 K (triangles) and 4 K (squares). The solid lines are the fits obtained with the expressions discussed in the text. The different contributions to the total absorption coefficient at 4 K are also reported.

4. Experimental

The bulk samples were prepared by high temperature oxidation (930–1150 °C) of a copper sheet in a furnace under N_2 flux. The surface of these samples was treated with a chemical etching of about 15 s in a KCl saturated 7 M HNO_3 solution, followed by a second etching in HNO_3 (69%) for 15 s. The samples were then dipped in deionized water and dried in N_2 flux. Resulting samples, with a final thickness of about 150 μm, can be used to measure absorption coefficients lower than about 600 cm^{-1} ($E < 2.05$ eV).

In order to study the optical properties of cuprous oxide at higher energies, thin films of about 1.5 μm of thickness were deposited on soda-lime glass substrates (Corning 2947) by RF-magnetron sputtering in a customized Leybold Z400 system at 500 °C, using an argon atmosphere ($P_{Ar} = 10^{-3}$ mbar) with an oxygen partial pressure of about 2.7×10^{-4} mbar.

The film thickness of all specimens was measured by a Dektak III stylus profilometer and X-ray diffraction (XRD) data were collected on a four-circle PANalytical X'Pert MRD diffractometer. The samples showed a single phase, polycrystalline Cu_2O.

The absorption coefficient of our samples has been obtained from spectrophotometric measurements using a PerkinElmer Lambda 9 with an integrating sphere in the wavelength range from 300 to 2500 nm. In the case of bulk samples no interference effects are present but multiple reflections inside the material must be considered. The measured transmittance $\tilde{T}$ and reflectance $\tilde{R}$ are linked to absorption coefficient and to the single surface reflectance R of the material by the following relations:

$$\tilde{T} = \frac{I_{transm}}{I_0} = \frac{(1-R)^2 e^{-\alpha d}}{1-R^2 e^{-2\alpha d}}, \tag{22}$$

$$\tilde{R} = \frac{I_{refl}}{I_0} = R\left(1 + \frac{(1-R)^2 e^{-2\alpha d}}{1-R^2 e^{-2\alpha d}}\right), \tag{23}$$

where I_0 is the total intensity of incident light and d is the sample's thickness. Using Eqs. (22) and (23), it is possible to express the absorption coefficient as a function of the directly measurable quantity $\tilde{T}$ and $\tilde{R}$:

$$\alpha = -\frac{1}{d}\log\left(\frac{1+\tilde{R}^2-2\tilde{R}-\tilde{T}^2+\sqrt{(1+\tilde{R}^2-2\tilde{R}-\tilde{T}^2)^2+4\tilde{T}^2}}{2\tilde{T}}\right) \tag{24}$$

which we used to obtain $\alpha(\hbar\omega)$ from the measured transmittance and reflectance spectra.

The case of thin films is more complicated because of the presence of several interference fringes which have to be removed to perform a good analysis. For this task we developed a numerical program based on the Swanepoel theory [30], which is able to provide the optical constant η and κ of the material, once the transmittance spectrum is known.

The absorption coefficient, as obtained by us or reported in the literature, invariably shows a non-zero value for energies well below the gap. For the bulk samples this background is of the order of a few tens of cm^{-1} while for the thin film it can reach many hundreds of cm^{-1}. The simplest explanation for this result is that it is due to defect absorption. To compare the intrinsic absorption at room temperature in different samples we have therefore subtracted to the data the absorption coefficient at 1.93 eV.

5. Results and discussion

The absorption spectra for a bulk sample ($d=150$ μm) and a thin film ($d=1.66$ μm) are shown in Fig. 2. The experimental absorption coefficient of our bulk sample overlaps with the room temperature data of Grun et al. [26] and both are in fairly good agreement with the literature data from Pastrňák [31] obtained at higher energies. Our data for the thin film, after the background correction, also nicely fit the bulk data thus confirming the Pastrňák absorption values in the energy range 2.1–2.4 eV. Finally, in Fig. 2 we have also reported the low energy tail of the absorption coefficient spectrum obtained by ellipsometry measurements [12]. At low energies these data are noisy and less reliable than the spectrophotometric ones and we decided to rely on them only for energies larger than 2.6 eV.

These room temperature data have been fitted using the same approach as that adopted for the low temperature ones. Since the excitonic peaks are completely smoothed out, the pseudo and the true continuous contributions by direct forbidden transition of the yellow and the green excitons have been evaluated according to Eqs. (12) and (16), with the same A values used at low temperatures $A^y=78.5\ cm^{-1}$ and $A^g=1115\ cm^{-1}$.

As for the low temperature data, we included in the fit the indirect transitions to the 1s yellow level involving the 13.6 meV Γ_{12}^- and 82 meV Γ_{15}^- phonons, and those to the 1s green level involving the 13.6 meV Γ_{12}^- and 43.4 meV Γ_2^- phonons. It must be noted that for this last process we included only the process with the phonon emission as the similar process where the 43.4 meV Γ_2^- phonon is instead absorbed is considerably weaker, owing to Eq. (20) and to a much larger value of the denominator in Eq. (18). To further improve the fit quality we have introduced a broadening of the indirect transitions to the 1s green exciton level by convoluting the square root function with a gaussian with a 25 meV variance.

We have found that the increase in the absorption coefficient with increasing temperature cannot be due to the increase in the phonon number only. To fit our data, we still use Eqs. (19) and (20) but we are forced to use, for indirect transitions to the 1s green level (and particularly for the process involving the 43.4 meV Γ_2^- phonon), a value of the constant C which increases with T. A value independent from T can be used instead for the indirect transitions to the 1s yellow level (see Table 1). The reason for this difference is not clear, but it could be due to a weak energy dependence of the terms in the denominator of Eq. (18), which produces a value closer to zero at room temperature.

The increase in slope observed in our data for energies higher than 2.4 eV has to be attributed to the blue and violet exciton series contributions. Indeed for these two excitonic bands the transitions are not forbidden and therefore the contributions from the $n=1$ peaks must be taken into account. The energies of these two peaks are 2.594 and 2.708 eV, respectively, as obtained from Ito ellipsometry measurements [12] also reported in the figure. However, it should be noted that Ito's analysis, based on peaks with a Lorentzian shape, cannot give the right behavior for α at low energy, predicting too high values that do not match with the curve from the spectrophotometric measurements. In order to obtain a reasonable behavior of the absorption coefficient at low energy, it is necessary to use a peak shape with an exponential

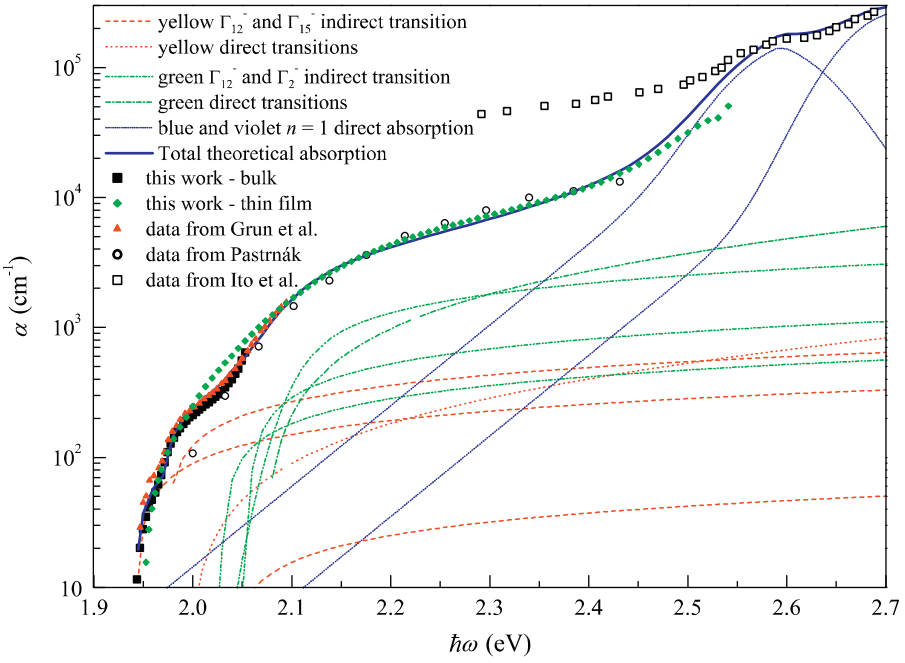

Fig. 2. Absorption coefficient data obtained on bulk and thin film Cu_2O samples compared with different literature data (Grun et al. [26], Pastrňák [31] and Ito et al. [12]). The solid line is the fit obtained with the expressions discussed in the text. The different contributions due to direct and indirect transitions are also shown.

Table 2
Value of the refractive index η and extinction coefficient κ for the Cu_2O at room temperature.

λ (nm)	η	κ	λ (nm)	η	κ	λ (nm)	η	κ	λ (nm)	η	κ
250	1.774	1.53783	454	3.457	1.04230	576	3.065	0.01396	720	2.846	0
255	1.759	1.57772	456	3.517	1.03890	580	3.054	0.01236	740	2.829	0
260	1.756	1.64010	458	3.584	1.00774	584	3.044	0.01065	760	2.814	0
265	1.775	1.72078	460	3.637	0.94882	588	3.035	0.00885	780	2.800	0
270	1.824	1.81169	462	3.664	0.87794	590	3.030	0.00794	800	2.787	0
275	1.910	1.89951	464	3.666	0.81196	592	3.026	0.00705	820	2.776	0
280	2.032	1.96502	466	3.654	0.75872	594	3.021	0.00618	840	2.765	0
285	2.178	1.98831	468	3.638	0.71952	596	3.017	0.00536	860	2.756	0
290	2.321	1.95996	470	3.622	0.69230	598	3.013	0.00457	880	2.747	0
295	2.432	1.88929	472	3.612	0.67383	600	3.008	0.00391	900	2.739	0
300	2.498	1.80266	474	3.611	0.65934	602	3.004	0.00336	950	2.721	0
305	2.520	1.72664	476	3.621	0.64242	603	3.002	0.00312	1000	2.705	0
310	2.517	1.67650	478	3.637	0.61431	604	3.000	0.00288	1050	2.692	0
315	2.503	1.65717	480	3.649	0.57334	606	2.996	0.00251	1100	2.681	0
320	2.494	1.66565	482	3.651	0.52433	608	2.992	0.00224	1150	2.672	0
325	2.499	1.69633	484	3.639	0.47481	610	2.988	0.00195	1200	2.663	0
330	2.526	1.74107	486	3.619	0.40878	611	2.987	0.00182	1250	2.655	0
335	2.578	1.78958	488	3.594	0.34678	612	2.985	0.00173	1300	2.649	0
340	2.656	1.83198	490	3.568	0.29052	614	2.981	0.00156	1350	2.643	0
345	2.756	1.85755	492	3.541	0.24130	616	2.977	0.00143	1400	2.637	0
350	2.870	1.85857	494	3.515	0.19973	618	2.974	0.00130	1450	2.632	0
355	2.986	1.83088	496	3.491	0.16573	620	2.970	0.00116	1500	2.628	0
360	3.095	1.77617	498	3.468	0.13865	622	2.967	0.00103	1550	2.624	0
365	3.186	1.70063	500	3.446	0.11749	624	2.963	9.044×10^{-4}	1600	2.620	0
370	3.255	1.61380	504	3.406	0.08858	626	2.960	7.568×10^{-4}	1650	2.617	0
375	3.302	1.52371	508	3.371	0.07112	627	2.958	6.637×10^{-4}	1700	2.613	0
380	3.331	1.43728	512	3.340	0.05985	628	2.957	5.352×10^{-4}	1750	2.610	0
385	3.345	1.35815	516	3.312	0.05189	629	2.955	3.692×10^{-4}	1800	2.608	0
390	3.350	1.28858	520	3.286	0.04586	630	2.953	3.488×10^{-4}	1850	2.605	0
395	3.348	1.22840	524	3.262	0.04109	632	2.950	3.044×10^{-4}	1900	2.603	0
400	3.343	1.17743	528	3.241	0.03720	634	2.947	2.525×10^{-4}	1950	2.601	0
405	3.336	1.13445	532	3.221	0.03396	636	2.944	1.854×10^{-4}	2000	2.599	0
410	3.330	1.09821	536	3.202	0.03121	637	2.942	1.374×10^{-4}	2050	2.597	0
415	3.325	1.06801	540	3.184	0.02883	638	2.941	3.713×10^{-5}	2100	2.595	0
420	3.321	1.04278	544	3.168	0.02673	640	2.938	0	2150	2.593	0
425	3.320	1.02239	548	3.153	0.02484	650	2.924	0	2200	2.592	0
430	3.321	1.00602	552	3.138	0.02310	660	2.910	0	2250	2.590	0
435	3.325	0.99452	556	3.124	0.02148	670	2.898	0	2300	2.589	0
440	3.332	0.98985	560	3.111	0.01993	680	2.886	0	2350	2.587	0
445	3.347	0.99684	564	3.099	0.01843	690	2.875	0	2400	2.586	0
450	3.385	1.01950	568	3.087	0.01696	700	2.865	0	2450	2.585	0
452	3.414	1.03231	572	3.075	0.01548	710	2.855	0	2500	2.584	0

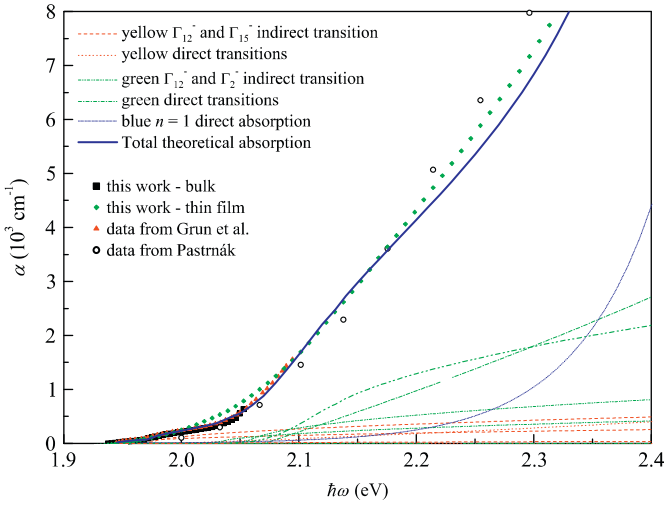

Fig. 3. Linear plot of the absorption coefficient data obtained on bulk and thin film Cu_2O together with the literature data by Grun et al. [26] and Pastrňák [31]. The solid line is the fit obtained with the expressions discussed in the text. The different contributions due to direct and indirect transitions are also shown.

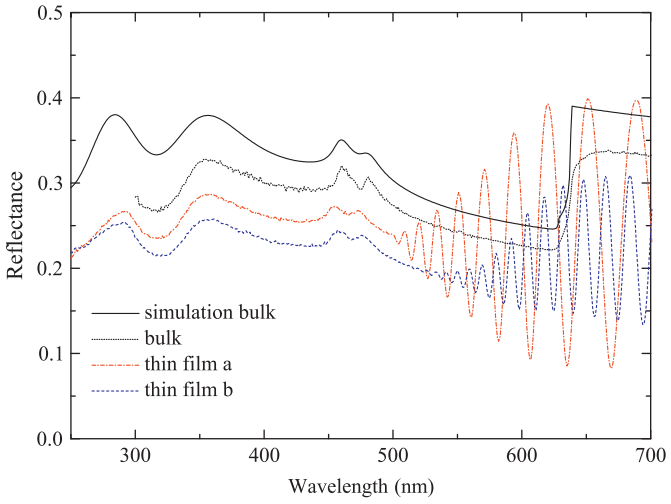

Fig. 4. Experimental reflectance measured on bulk and two thin films ($d=1.66$ and $d=3.30$ μm) of Cu_2O. The theoretical reflectance calculated using the optical constants of Table 2 is also reported for comparison (solid line).

tail. This behavior is a quite common feature of the excitonic absorption edge [32] and many different theories were proposed to explain it [33]. A very refined theory for the shape of the exciton peak was developed by Dow and Redfield [34,35] but its solution cannot be given with a simple analytical formula. Therefore, we simply use the sum of a gaussian peak and of an

exponential decay $e^{-|(E-E_0)/E_u|}$ where E_0 is the peak energy and E_u is the characteristic energy of the Urbach tail. A good fit is obtained using $E_u = 70$ meV: the result of the fit is shown in Fig. 2, where the different theoretical contributions to the total absorption arising from the different absorption mechanisms discussed hitherto are also reported.

The room temperature Cu_2O optical constants are reported in a tabular form in Table 2. The $\alpha(\hbar\omega)$ expression developed in this work has been used to calculate the κ values in the energy range 1.943−2.56 eV, while for energies higher than 2.56 eV and for the η values in the whole energy range the expressions reported in the paper by Ito et al. were used.

In Fig. 3 the same data of Fig. 2 are reported on a linear scale to show that in the energy range 2.1–2.3 eV the absorption coefficient follows a nearly linear trend. This is an accidental result since it is produced by the superposition of many different contributions. There is no energy range where a different power behavior (1/2, 2/3 or 2) can be clearly observed.

A fit of the absorption coefficient with any expression of the form $(E-E_g)^r$ is therefore not a reliable way to determine the gap of a Cu_2O sample. A simpler way to check whether a sample is made of Cu_2O or not is to measure its reflectance at energies larger than 2.5 eV. Indeed, two peaks in the reflectance at about 2.59 eV and 2.7 eV, corresponding to the direct allowed transitions to the $n=1$ exciton levels of the blue and violet series, should be clearly visible. This is demonstrated in Fig. 4, where the experimental reflectance spectra of a Cu_2O bulk and of two thin film samples are reported, together with the theoretical one calculated using the optical constants η and κ reported in Table 2.

It should be noted that these two peaks do not appear in samples of low quality (for example those deposited at low temperature or heavily doped), and moreover they do not shift rigidly with the fundamental gap, neither upon temperature variation [36] nor upon alloying effects. The latter feature is the subject of an ongoing research work, to be presented elsewhere. As a concluding remark, the lower reflectance observed in experimental data of Fig. 4 with respect to the theoretical prediction is probably due to light losses induced by the surface roughness, which are larger in as-grown thin films than in well etched bulk samples.

Acknowledgments

C. Malerba gratefully acknowledges a research grant within the project "Modified copper oxide for high efficiency photovoltaic cells" funded by Fondazione Cassa di Risparmio di Trento e Rovereto.

References

[1] C.-C. Hu, J.-N. Nian, H. Teng, Electrodeposited p-type Cu_2O as photocatalyst for h_2 evolution from water reduction in the presence of WO_3, Sol. Energy Mater. Sol. Cells 92 (2008) 1071–1076.
[2] X. Zou, G. Fang, L. Yuan, M. Li, W. Guan, X. Zhao, Top-gate low-threshold voltage p-Cu_2O thin-film transistor grown on SiO_2/Si substrate using a high-κ HfON gate dielectric, IEEE Electron Device Lett. 31 (2010) 827–829.
[3] S.-O. Kang, S. Hong, J. Choi, J.-S. Kim, I. Hwang, I.-S. Byun, K.-S. Yun, B.H. Park, Electrochemical growth and resistive switching of flat-surfaced and (111)-oriented Cu_2O films, Appl. Phys. Lett. 95 (2009) 092108.
[4] C.Y. Lam, K.H. Wong, Characteristics of heteroepitaxial $Cu_{2-x}Mn_xO$/Nb-$SrTiO_3$ p-n junction, J. Non-Cryst. Solids 354 (2008) 4262–4266.
[5] A. Mittiga, E. Salza, F. Sarto, M. Tucci, R. Vasanthi, Heterojunction solar cell with 2% efficiency based on a Cu_2O substrate, Appl. Phys. Lett. 88 (2006) 163502 .
[6] K. Akimoto, S. Ishizuka, M. Yanagita, Y. Nawa, G.K. Paul, T. Sakurai, Thin film deposition of Cu_2O and application for solar cells, Sol. Energy 80 (2006) 715–722.
[7] S.S. Jeong, A. Mittiga, E. Salza, A. Masci, S. Passerini, Electrodeposited ZnO/Cu_2O heterojunction solar cells, Electrochim. Acta 53 (2008) 2226–2231.
[8] S. Nikitine, J.B. Grun, M. Sieskind, Etude spectrophotometrique de la serie jaune de Cu_2O aux basses temperatures, J. Phys. Chem. Solids 17 (1961) 292–300.
[9] J.B. Grun, M. Sieskind, S. Nikitine, Détermination de l'intensité d'oscillateur des raies de la série verte de Cu_2O aux basses températures, J. Phys. Radium 22 (1961) 176–178.
[10] A. Daunois, J.L. Deiss, B. Meyer, Étude spectrophotométrique de l'absorption bleue et violette de Cu_2O, J. Phys. 27 (1966) 142–146.
[11] R.J. Elliott, Intensity of optical absorption by excitons, Phys. Rev. 108 (1957) 1384–1389.
[12] T. Ito, T. Kawashima, H. Yamaguchi, T. Masumi, S. Adachi, Optical properties of Cu_2O studied by spectroscopic ellipsometry, J. Phys. Soc. Jpn. 67 (1998) 2125–2131.
[13] B. Balamurugan, B.R. Mehta, Optical and structural properties of nanocrystalline copper oxide thin films prepared by activated reactive evaporation, Thin Solid Films 396 (2001) 90–96.
[14] M.F. Al-Kuhaili, Characterization of copper oxide thin films deposited by the thermal evaporation of cuprous oxide (Cu_2O), Vacuum 82 (2008) 623–629.
[15] C. Uihlein, D. Fröhlich, R. Kenklies, Investigation of exciton fine structure in Cu_2O, Phys. Rev. B 23 (1981) 2731–2740.
[16] R.J. Elliott, Theory of the exciton spectra in Cu_2O, in: Proceedings of the International Conference on Semiconductor Physics (fifth ed., Prague, 1960), 1961, pp. 408–410.
[17] R. Elliott, Symmetry of excitons in Cu_2O, Phys. Rev. 124 (1961) 340–345.
[18] T. Itoh, S.-I. Narita, Study of absorption spectra of excitons in Cu_2O by wavelength modulation technique, J. Phys. Soc. Jpn. 39 (1975) 132–139.
[19] R.A. Forman, W.S. Brower Jr., H.S. Parker, Phonons and the green exciton series in cuprous oxide, Cu_2O, Phys. Lett. A 36 (1971) 395–396.
[20] V.T. Agekyan, Spectroscopic properties of semiconductor crystals with direct forbidden energy gap, Phys. Status Solidi A 43 (1977) 11.
[21] M. Matsuura, H. Büttner, Optical properties of excitons in polar semiconductors: energies, oscillator strengths, and phonon side bands, Phys. Rev. B 21 (1980) 679–691.
[22] T. Ueno, On the contour of the absorption lines in Cu_2O, J. Phys. Soc. Jpn. 26 (1969) 438–446.
[23] K. Shindo, T. Goto, T. Anzai, Exciton-LO phonon scattering in Cu_2O, J. Phys. Soc. Jpn. 36 (1974) 753–758.
[24] J.B. Grun, S. Nikitine, Étude de la forme des raies des séries jaune et verte de la cuprite, J. Phys. 24 (1963) 355–358.
[25] Y. Toyozawa, Interband effect of lattice vibrations in the exciton absorption spectra, J. Phys. Chem. Solids 25 (1964) 59–71.
[26] J.B. Grun, M. Sieskind, S. Nikitine, Étude spectrophotométrique des spectres continus de Cu_2O a diverses temperatures, J. Phys. Chem. Solids 19 (1961) 189–197.
[27] T. Itoh, S.-I. Narita, Analysis of wavelength derivative spectra of exciton in Cu_2O, J. Phys. Soc. Jpn. 39 (1975) 140–147.
[28] J.L. Deiss, A. Daunois, S. Nikitine, Electroabsorption near the 1S line of the green series of Cu_2O, Solid State Commun. 9 (1971) 217–221.
[29] J.L. Deiss, J.B. Grun, S. Nikitine, Observation de deux raies faibles nouvelles dans le spectre de la cuprite à 4,2 °K. Essai d'interprétation, J. Phys. 24 (1963) 206–208.
[30] R. Swanepoel, Determination of the thickness and optical constants of amorphous silicon, J. Phys. E: Sci. Instrum. 16 (1983) 1214–1222.
[31] J. Pastrňák, Temperature dependence of light absorption in cuprous oxide crystals in the visible region of the spectrum, Sov. Phys. Sol. State 1 (1959) 888–891.
[32] M. Nagasawa, Urbach's rule exhibited in SnO_2, Solid State Commun. 7 (1969) 1731.
[33] H. Sumi, A. Sumi, The Urbach-Martienssen rule revisited, J. Phys. Soc. Jpn. 56 (1987) 2211.
[34] J.D. Dow, D. Redfield, Electroabsorption in semiconductors: the excitonic absorption edge, Phys. Rev. B 1 (1970) 3358.
[35] J.D. Dow, D. Redfield, Toward a unified theory of Urbach's rule and exponential absorption edges, Phys. Rev. B 5 (1972) 594.
[36] J.B. Grun, M. Sieskind, S. Nikitine, Étude de l'absorption et de la réflexion de la cuprite aux très basses températures dans le visible de courtes longueurs d'onde, J. Phys. Chem. Solids 21 (1961) 119–122.